

SUPPORTING INFORMATION

Lanthanide coordination polymers with 1,2-phenylenediacetate.

Insa Badiane^{a,b}, Stéphane Freslon^a, Yan Suffren^a, Carole Daiguebonne^a, Guillaume Calvez^a, Kevin Bernot^a, Magatte Camara^b and Olivier Guillou^a.

^a INSA Rennes, UMR 6226 "Institut des Sciences Chimiques de Rennes", F-35708 Rennes

^b Université Assane Seck de Ziguinchor, LCPM – Groupe "Matériaux Inorganiques: Chimie Douce et Cristallographie", BP. 523 Ziguinchor – Sénégal

,

Table S1. Crystal and final structure refinement data already reported.

Molecular formula	Nd ₂ C ₃₀ O ₁₆ H ₃₃	La ₂ C ₃₀ O ₁₆ H ₃₃	Tb ₂ C ₃₀ O ₁₆ H ₃₆	Ho ₂ C ₃₀ O ₁₆ H ₃₆	Er ₂ C ₃₀ O _{16.5} H ₃₃	Pr ₂ C ₃₀ O _{16.5} H ₃₃	Dy ₂ C ₃₀ O ₁₆ H ₃₂
System	Monoclinic	Monoclinic	Monoclinic	Monoclinic	Monoclinic	Monoclinic	Monoclinic
a (Å)	26.2906 (18)	26.271 (14)	26.2699 (4)	26.317 (4)	26.317 (3)	26.223 (7)	26.2718 (9)
b (Å)	16.1172 (11)	16.149 (8)	16.0274 (2)	16.004 (3)	16.1589 (19)	16.097 (4)	16.0042 (6)
c (Å)	7.8327 (5)	7.966 (4)	7.6724 (1)	7.6263 (12)	7.8459 (9)	7.852 (2)	7.6441 (3)
β (°)	93.173 (5)	92.850 (9)	93.345 (1)	93.471 (2)	93.124 (2)	93.031 (4)	93.389 (2)
V (Å ³)	3313.9 (4)	3375 (3)	3224.87 (8)	3206.1 (9)	3331.6 (7)	3309.8 (15)	3208.41 (20)
Z	4	4	4	4	4	4	4
Formula weight (g mol ⁻¹)	937.04	926.38	958.36	978.42	992.08	939.38	973.56
Space group (No.)	C2/c (n°15)	C2/c (n°15)	C2/c (n°15)				
D _{calc} (g cm ⁻³)	1.878	1.823	1.97	2.027	1.978	1.885	2.01538
μ (mm ⁻¹)	3.173	2.570	4.426	4.976	5.08	2.99	4.70
R (%)	1.75	5.05	2.94	3.30	1.4	1.9	2.2
R _w (%)	10.357	13.315	8.04	12.4	11.3	10	5.5
GoF	1.053	1.055	1.003	1.069	1.09	1.081	1.06
N° CCDC	953279	952811	635048	635081	963497	963495	669663
Reference	44	44	47	47	46	46	45

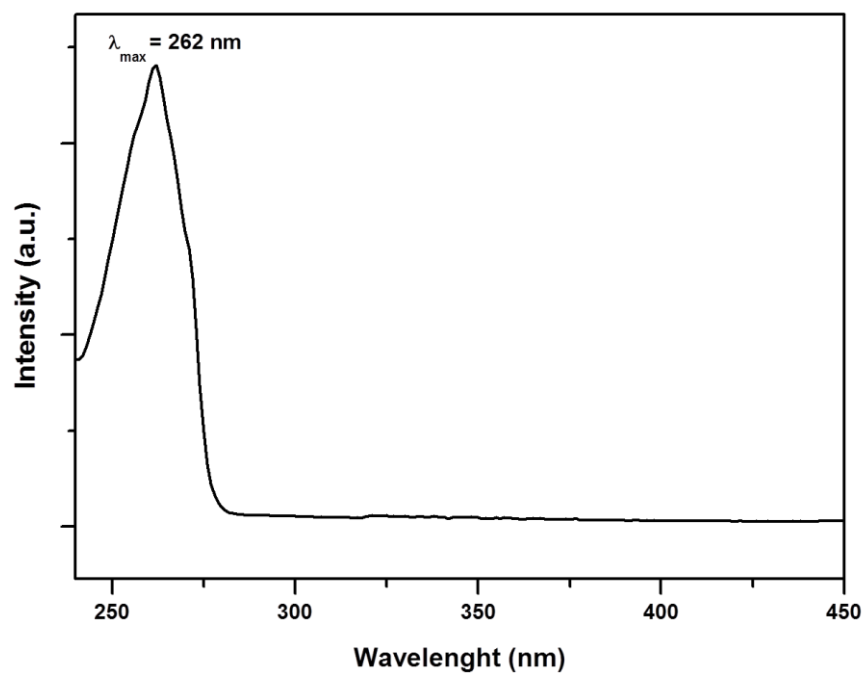


Figure S1. UV-vis absorption spectrum of an aqueous solution of Na₂O-pda ($c = 4.3 \cdot 10^{-5} \text{ mol.L}^{-1}$).

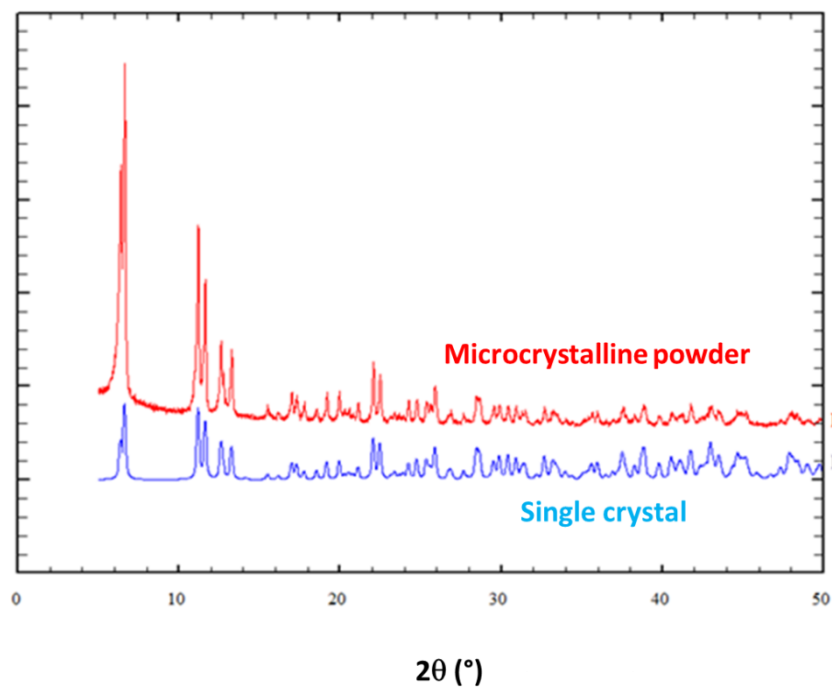


Figure S2. Experimental and simulated (on the basis of crystal structure) powder diffraction patterns of $[\text{La}_2(\text{o-pda})_3(\text{H}_2\text{O})_4] \cdot 4\text{H}_2\text{O}$ (**1**).

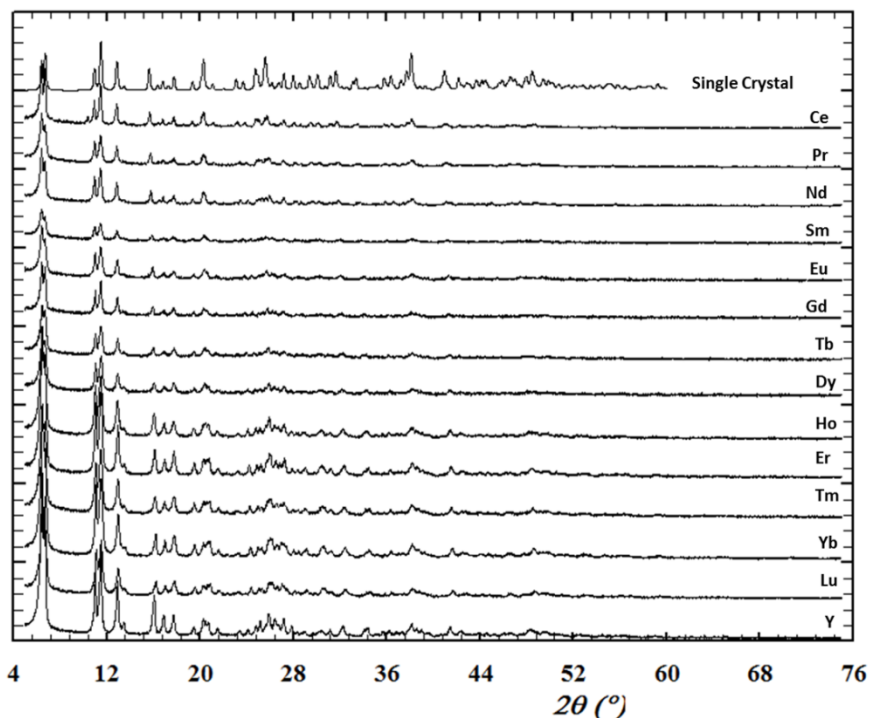


Figure S3. Experimental and simulated (on the basis of the crystal structure from reference [47]) powder X-ray diffraction patterns of **microcrystalline** compounds $[\text{Ln}_2(\text{o-pda})_3(\text{H}_2\text{O})_2, 2\text{H}_2\text{O}]_\infty$ for $\text{Ln} = \text{Ce-Nd, Sm-Lu}$ and Y (**2**).

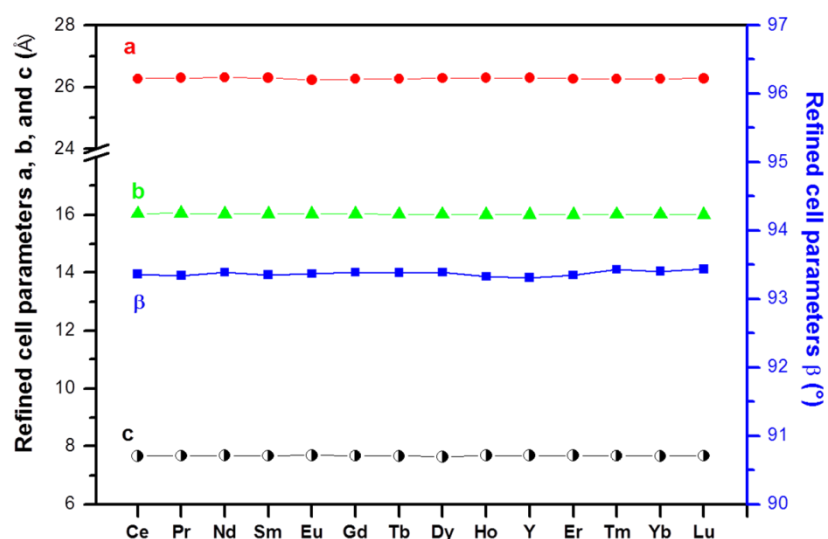


Figure S4. Refined cell parameters for **microcrystalline** compounds $[\text{Ln}_2(\text{o-pda})_3(\text{H}_2\text{O})_2, 2\text{H}_2\text{O}]_\infty$ for $\text{Ln} = \text{Ce-Nd, Sm-Lu}$ and Y (**2**).

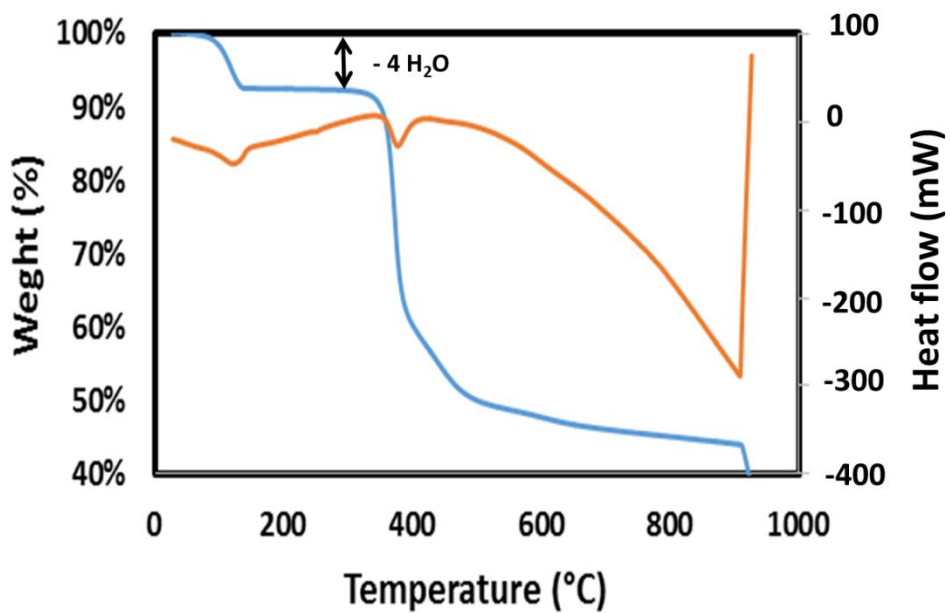


Figure S5. Thermal analyzes of microcrystalline $[\text{Gd}_2(\text{o-pda})_3(\text{H}_2\text{O})_2,2\text{H}_2\text{O}]_\infty$.

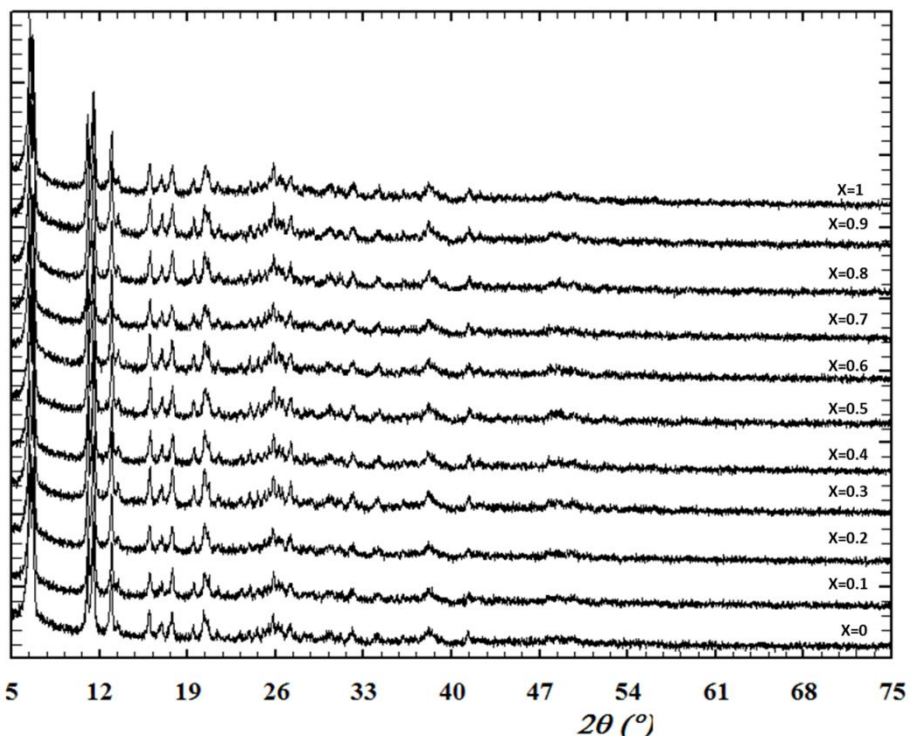


Figure S6. Powder X-ray diffraction diagrams for microcrystalline $[\text{Tb}_{2-2x}\text{Gd}_{2x}(\text{o-pda})_3(\text{H}_2\text{O})_2,2\text{H}_2\text{O}]_\infty$ with $0 \leq x \leq 0.9$.

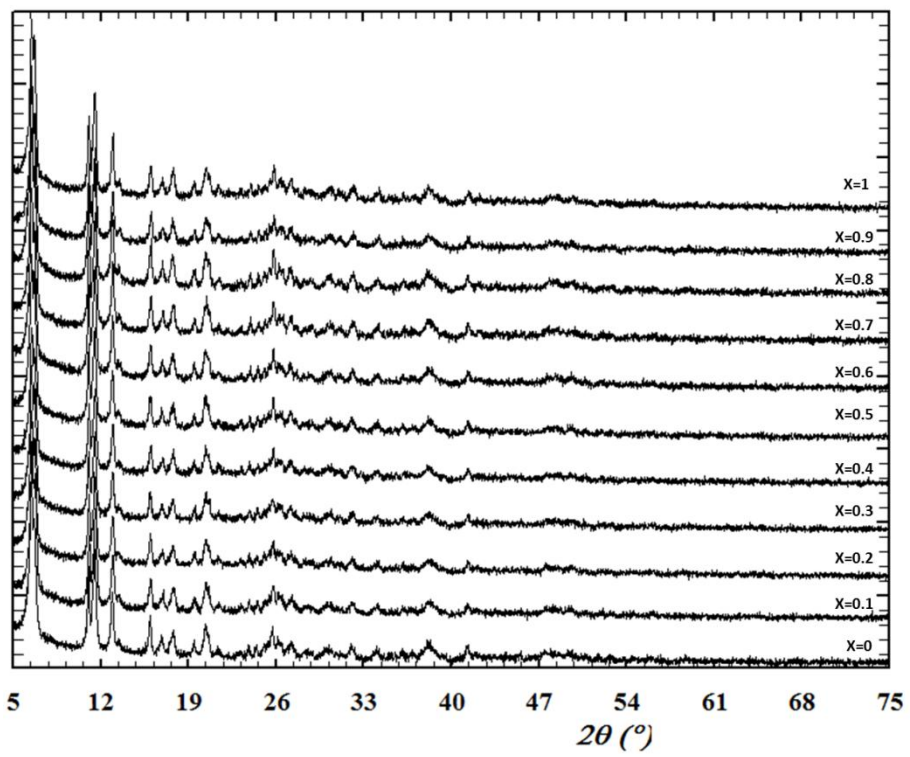


Figure S7. Powder X-ray diffraction diagrams for microcrystalline $[\text{Tb}_{2-x}\text{Eu}_{2x}(\text{o-pda})_3(\text{H}_2\text{O})_2, 2\text{H}_2\text{O}]_\infty$ with $0 \leq x \leq 0.9$.

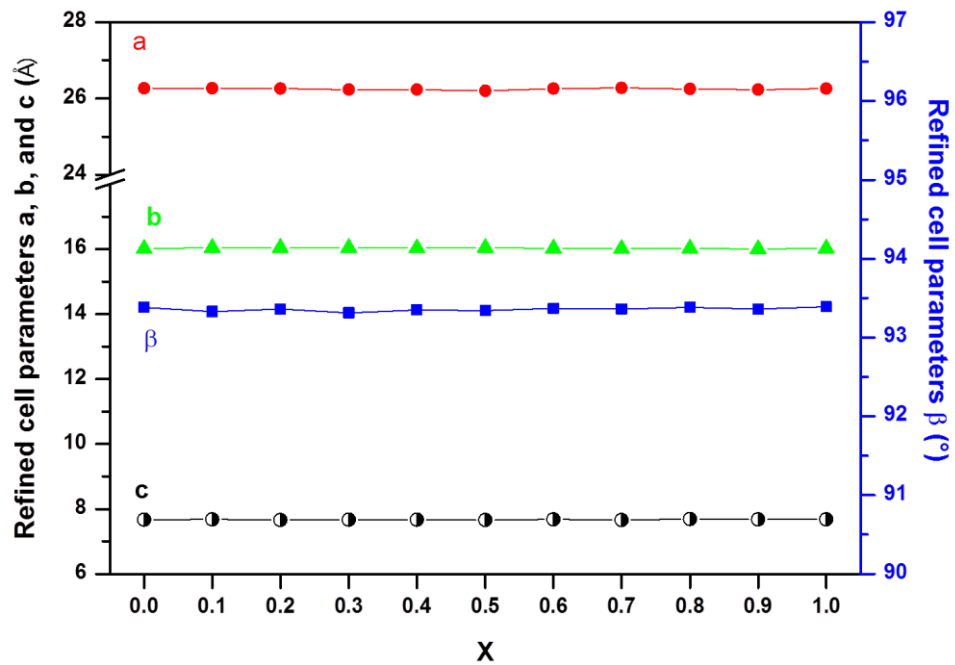


Figure S8. Refined cell parameters for microcrystalline $[\text{Tb}_{2-x}\text{Gd}_{2x}(\text{o-pda})_3(\text{H}_2\text{O})_2, 2\text{H}_2\text{O}]_\infty$ with $0 \leq x \leq 0.9$.

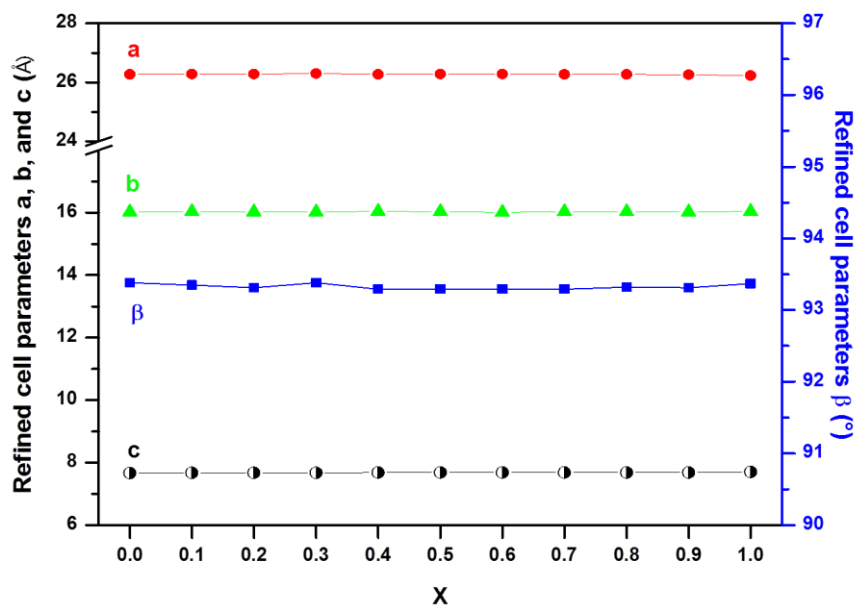


Figure S9. Refined cell parameters for microcrystalline $[\text{Tb}_{2-x}\text{Eu}_{2x}(\text{o-pda})_3(\text{H}_2\text{O})_2,2\text{H}_2\text{O}]_\infty$ with $0 \leq x \leq 0.9$.

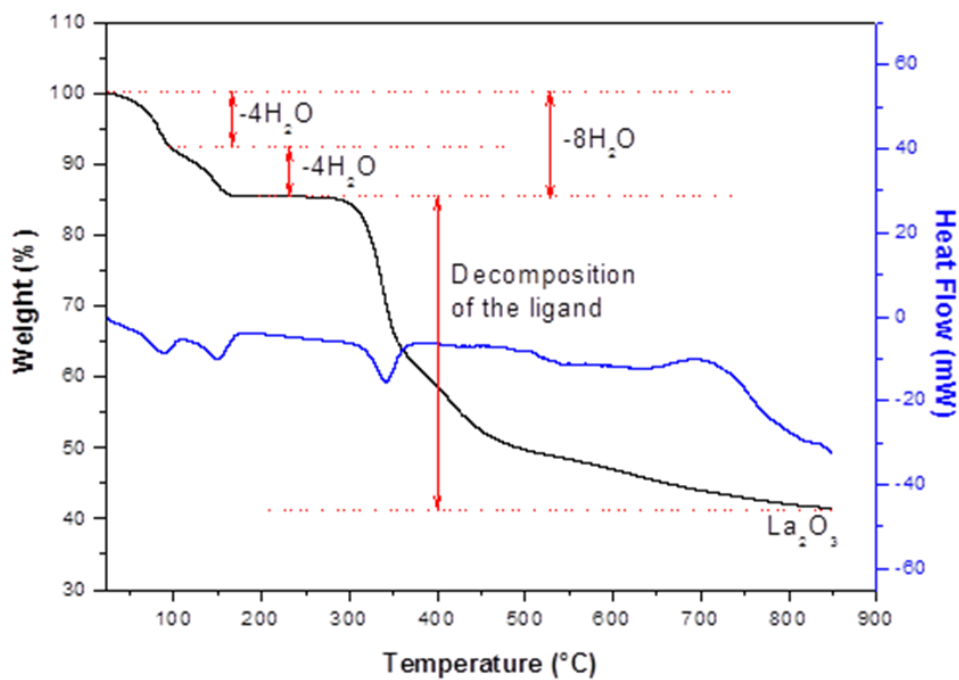


Figure S10. Thermal analyzes of microcrystalline $[\text{La}_2(\text{o-pda})_3(\text{H}_2\text{O})_4,4\text{H}_2\text{O}]_\infty$ (**1**).

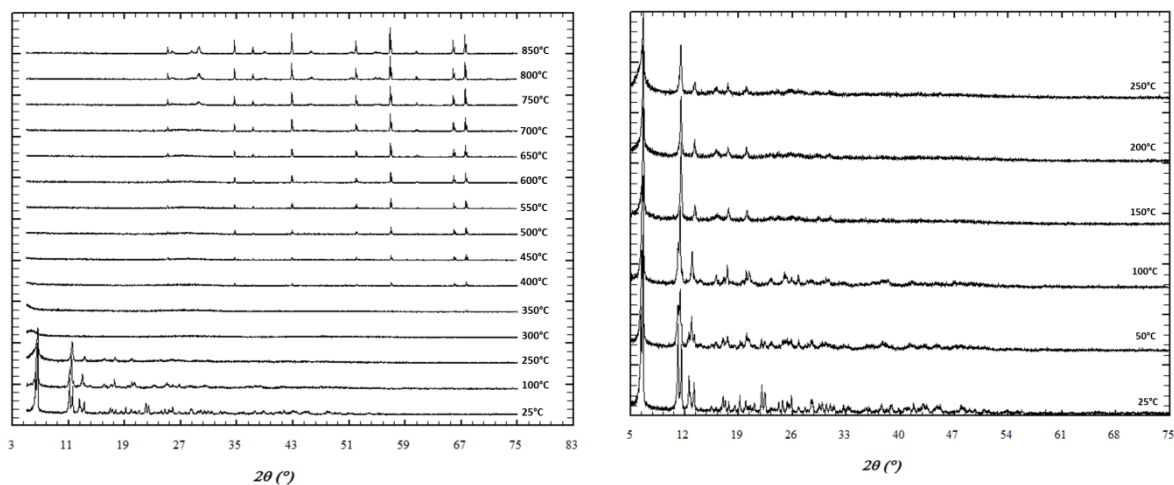


Figure S11. Temperature-dependent X-ray powder diffraction of microcrystalline $[\text{La}_2(\text{o-pda})_3(\text{H}_2\text{O})_4,4\text{H}_2\text{O}]_\infty$ (**1**).

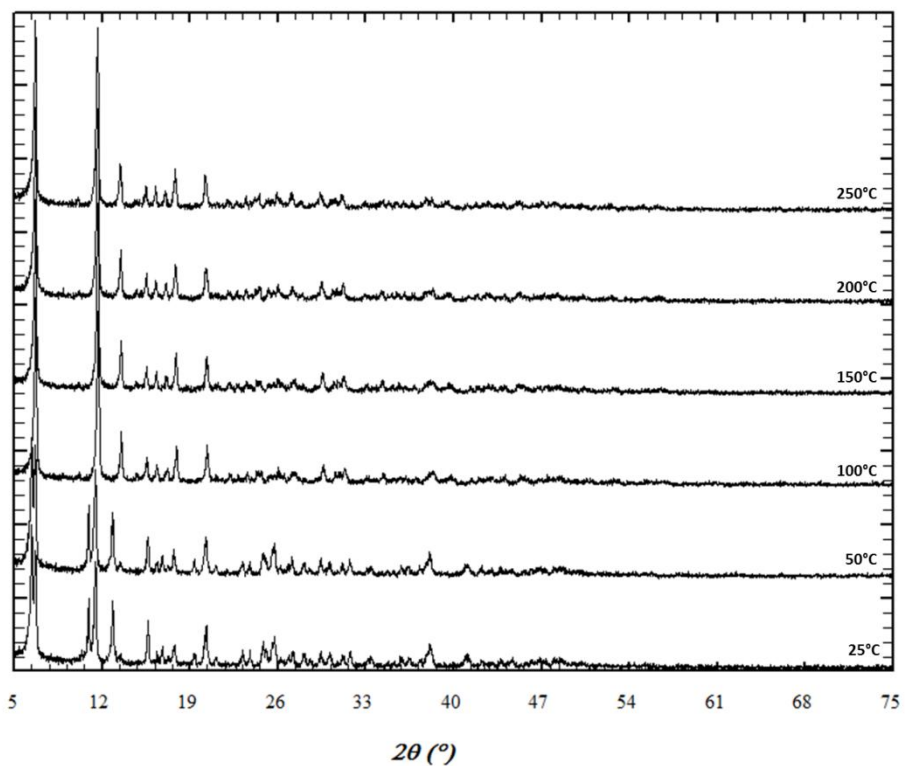


Figure S12. Temperature-dependent powder X-ray diffraction diagrams of microcrystalline $[\text{Gd}_2(\text{o-pda})_3(\text{H}_2\text{O})_2,2\text{H}_2\text{O}]_\infty$ between room temperature and 250°C under nitrogen atmosphere.

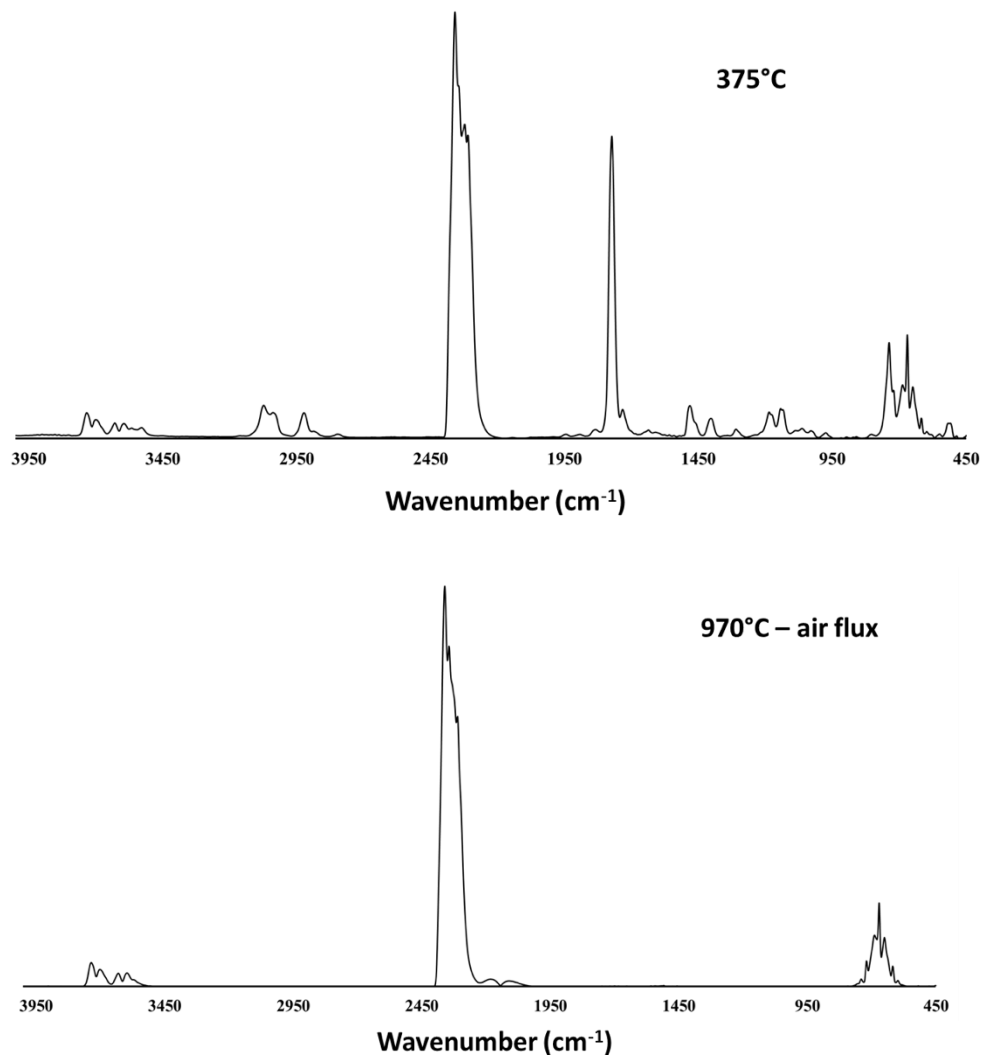


Figure S13. IR spectrum of microcrystalline $[\text{Gd}_2(\text{o-pda})_3(\text{H}_2\text{O})_2, 2\text{H}_2\text{O}]_\infty$ recorded at 375°C (N_2 flux) and 970°C (air flux).

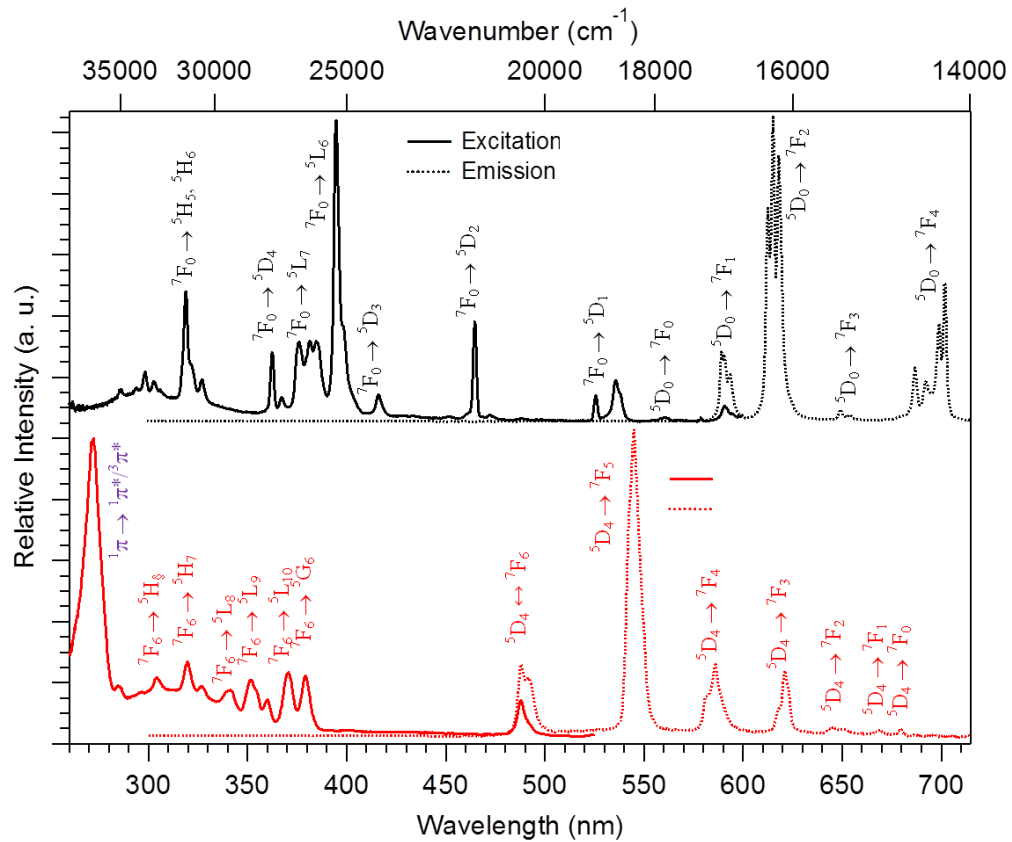


Figure S14. Top: Excitation ($\lambda_{\text{em}} = 615$ nm) and emission ($\lambda_{\text{exc}} = 395$ nm) spectra for microcrystalline $[\text{Eu}_2(\text{o-pda})_3(\text{H}_2\text{O})_2, 2\text{H}_2\text{O}]_\infty$. Bottom: Excitation ($\lambda_{\text{em}} = 545$ nm) and emission ($\lambda_{\text{exc}} = 379$ nm) spectra for microcrystalline $[\text{Tb}_2(\text{o-pda})_3(\text{H}_2\text{O})_2, 2\text{H}_2\text{O}]_\infty$.

Table S2. Chemical analyzes for compounds that constitute families (1) and (2).

Chemical formula	MW (g.mol ⁻¹)	%C calc. (found)	%H calc. (found)	%O calc. (found)	%Ln calc. (found)
$[\text{La}_2(\text{o-pda})_3(\text{H}_2\text{O})_4, 4\text{H}_2\text{O}]_\infty$	998.45	36.1 (36.0)	4.0 (4.1)	32.1 (32.2)	27.8 (27.7)
$[\text{Ce}_2(\text{o-pda})_3(\text{H}_2\text{O})_2, 2\text{H}_2\text{O}]_\infty$	928.81	38.8 (39.0)	3.5 (3.5)	27.6 (27.6)	30.1 (29.9)
$[\text{Pr}_2(\text{o-pda})_3(\text{H}_2\text{O})_2, 2\text{H}_2\text{O}]_\infty$	930.39	38.7 (38.7)	3.5 (3.4)	27.5 (27.4)	30.3 (30.5)
$[\text{Nd}_2(\text{o-pda})_3(\text{H}_2\text{O})_2, 2\text{H}_2\text{O}]_\infty$	937.05	38.5 (38.7)	3.4 (3.5)	27.3 (27.0)	30.8 (30.8)
$[\text{Sm}_2(\text{o-pda})_3(\text{H}_2\text{O})_2, 2\text{H}_2\text{O}]_\infty$	949.29	38.0 (38.2)	3.4 (3.3)	27.0 (27.0)	31.6 (31.5)
$[\text{Eu}_2(\text{o-pda})_3(\text{H}_2\text{O})_2, 2\text{H}_2\text{O}]_\infty$	952.50	37.8 (37.8)	3.4 (3.4)	26.9 (27.0)	31.9 (31.8)
$[\text{Gd}_2(\text{o-pda})_3(\text{H}_2\text{O})_2, 2\text{H}_2\text{O}]_\infty$	963.07	37.4 (37.4)	3.3 (3.5)	26.6 (26.4)	32.7 (32.7)
$[\text{Tb}_2(\text{o-pda})_3(\text{H}_2\text{O})_2, 2\text{H}_2\text{O}]_\infty$	966.43	37.3 (37.5)	3.3 (3.1)	26.5 (26.4)	32.9 (33.0)
$[\text{Dy}_2(\text{o-pda})_3(\text{H}_2\text{O})_2, 2\text{H}_2\text{O}]_\infty$	973.57	37.0 (36.9)	3.3 (3.3)	26.3 (26.2)	33.4 (33.6)
$[\text{Ho}_2(\text{o-pda})_3(\text{H}_2\text{O})_2, 2\text{H}_2\text{O}]_\infty$	978.44	36.8 (36.9)	3.3 (3.4)	26.2 (26.3)	33.7 (33.4)
$[\text{Er}_2(\text{o-pda})_3(\text{H}_2\text{O})_2, 2\text{H}_2\text{O}]_\infty$	983.09	36.7 (36.5)	3.3 (3.3)	26.0 (26.2)	34.0 (34.0)
$[\text{Tm}_2(\text{o-pda})_3(\text{H}_2\text{O})_2, 2\text{H}_2\text{O}]_\infty$	986.44	36.5 (36.5)	3.3 (3.4)	25.9 (25.8)	34.3 (34.3)
$[\text{Yb}_2(\text{o-pda})_3(\text{H}_2\text{O})_2, 2\text{H}_2\text{O}]_\infty$	994.65	36.2 (36.0)	3.3 (3.1)	25.7 (25.9)	34.8 (35.0)
$[\text{Lu}_2(\text{o-pda})_3(\text{H}_2\text{O})_2, 2\text{H}_2\text{O}]_\infty$	998.51	36.1 (36.2)	3.2 (3.2)	25.6 (25.6)	35.1 (35.0)
$[\text{Y}_2(\text{o-pda})_3(\text{H}_2\text{O})_2, 2\text{H}_2\text{O}]_\infty$	826.39	43.6 (43.5)	3.9 (4.0)	31.0 (31.0)	21.5 (21.5)

Table S3. Relative lanthanide ratios for $[Tb_{2-x}Gd_{2x}(o\text{-pda})_3(H_2O)_2,2H_2O]_\infty$ with $0.1 \leq x \leq 0.9$

	% (expected)		% (measured)	
	Gd	Tb	Gd	Tb
x=0.9	90	10	86.4 ± 4	13.6 ± 4
x=0.8	80	20	83.7 ± 2	16.3 ± 2
x=0.7	70	30	72 ± 6	28 ± 6
x=0.6	60	40	64.7 ± 2	35.3 ± 2
x=0.5	50	50	52.3 ± 0.7	47.7 ± 0.7
x=0.4	40	60	43.4 ± 3	56.6 ± 3
x=0.3	30	70	30.8 ± 2	69.2 ± 2
x=0.2	20	80	20.4 ± 0.8	79.6 ± 0.8
x=0.1	10	90	10 ± 2	90 ± 2

Table S4. Relative lanthanide ratios for $[Tb_{2-x}Eu_{2x}(o\text{-pda})_3(H_2O)_2,2H_2O]_\infty$ with $0.1 \leq x \leq 0.9$

	% (expected)		% (measured)	
	Eu	Tb	Eu	Tb
x=0.9	90	10	91.4 ± 2	8.6 ± 2
x=0.8	80	20	81 ± 2	19 ± 2
x=0.7	70	30	74 ± 4	26 ± 4
x=0.6	60	40	62.3 ± 4	37.7 ± 4
x=0.5	50	50	48 ± 2	52 ± 2
x=0.4	40	60	43.3 ± 2	56.7 ± 2
x=0.3	30	70	31 ± 2	69 ± 2
x=0.2	20	80	17 ± 3	83 ± 3
x=0.1	10	90	12 ± 2	88 ± 2